Journal Pre-proof

Catalytic feasibility of Ce-doped $LaCoO_3$ systems for chlorobenzene oxidation: An analysis of the synthesis method

Héctor Acosta Pérez, Carlos A. López, Luis E. Cadús, Fabiola N. Agüero

PII: S1002-0721(21)00151-4

DOI: https://doi.org/10.1016/j.jre.2021.06.004

Reference: JRE 1022

To appear in: *Journal of Rare Earths*

Received Date: 4 February 2021

Revised Date: 3 June 2021

Accepted Date: 10 June 2021

Please cite this article as: Pérez HA, López CA, Cadús LE, Agüero FN, Catalytic feasibility of Ce-doped $LaCoO_3$ systems for chlorobenzene oxidation: An analysis of the synthesis method, *Journal of Rare Earths*, https://doi.org/10.1016/j.jre.2021.06.004.

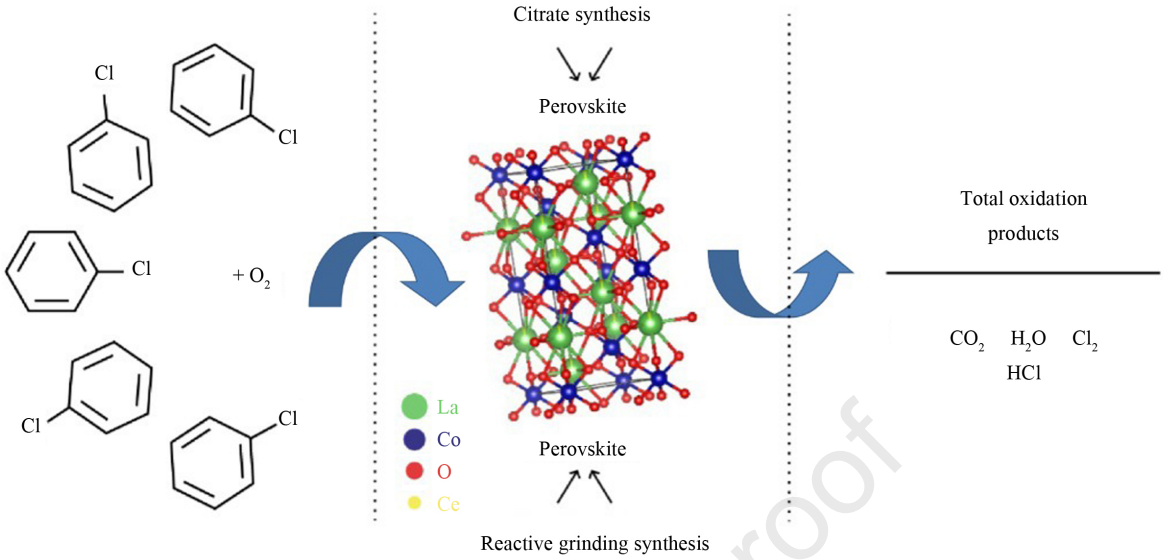

Catalytic feasibility of Ce-doped $LaCoO_3$ systems for chlorobenzene oxidation: An analysis of the synthesis method

Héctor Acosta Pérez, Carlos A. López, Luis E. Cadús, Fabiola N. Agüero*

Chemical Technology Research Institute (INTEQUI), UNSL - CONICET; Faculty of Biochemical Chemistry and Pharmacy (UNSL), Almirante Brown 1455, 5700 San Luis, Argentina

e-mail: fnaguero@unsl.edu.ar

Telephone: 54 (0266) 4520300 int 3148

Abstract

A family of Ce-doped $LaCoO_3$ perovskites are presented as possible catalyst for Cl-VOCs elimination. These materials with different contents of Ce are obtained through the citrate and the reactive grinding methods. The insertion of Ce in the original perovskite structure favours the presence of Co^{2+}/Co^{3+} and Ce^{3+}/Ce^{4+} redox pairs and a higher content of oxygen vacancies that enhances the catalytic performance in chlorobenzene combustion based in differential kinetics studies. The family obtained by the grinding method presents a performance as high as the synthesized by citrate method. Thus, the reactive grinding is a feasible green chemistry alternative to obtain a catalyst with the same performance than that obtained from traditional methods. Finally, the stability of samples was evaluated under total combustion reaction conditions showing an excellent activity during 45 h time on stream.

Keywords: Cl-VOCs, Perovskites; chlorobenzene; cerium; cobalt; Rare earths

1. Introduction

Chlorinated volatile organic compounds (Cl-VOCs) including polychloromethanes (PCMs), polychloroethanes (PCAs) and polychloroethylenes (PCEs), are widely used as solvents, degreasing agents and a variety of commercial products [1]. These contaminants are mainly regarded as persistants and resistant to biodegradation in the environment [2]. Cl-VOCs have been classified as hazardous gas pollutants and were included in the list of highly harmful chemicals targeted in the emission reduction efforts of most counties due to its toxicity and carcinogenic nature. Chlorobenzene is one of the chlorinated compounds from industrial processes which is usually used as model for Cl-VOC because it is a precursor or intermediate product of polychlorinated wastes [3,4]. A number of techniques have been used to eliminate chlorinated VOCs, and catalytic combustion is considered to be an efficient and low energy cost option [5,6].

Vanadium based catalysts [3,7], nobel metals (Pt, Pd Ru) supported on zeolites [7,8] and transition metal oxides [9–11] have been reported as catalysts used for the catalytic combustions of Cl-VOC. The use of noble metals is limited due to their high cost and low resistance to chlorine poisoning [12,13]. Transition metal oxides, including cobalt, manganese, copper and chromium, present not only a better thermal stability, a strong poisoning resistance and low costs but also enhance catalytic activity by the modification with rare earth elements [14,15]. Dai et al. [16] studied CeMnLa catalysts and presented a high catalytic activity, selectivity and stability at 350 °C. Yang et al. [17] reported the catalytic performance of mixed transition oxides of $CeMO_x$ (M: V, Cr, Mn, Fe, Co, Ni and Cu) for Cl-VOC combustion reaction. Moreover, Chen et al. [18] showed

that Co-Cu-Mn mixed oxide catalysts exhibited high catalytic activity in the oxidation of VOCs. Co_3O_4/La-CeO_2 catalyst was found to provide more adsorbed species and lattice oxygen species due to the interaction between Co^{3+}/Co^{2+} and Ce^{4+}/Ce^{3+} couples, which resulted in the enhancement in the catalytic activity.

Rare earth perovskites have been widely studied in Cl-VOCs oxidation due to the high structural and thermal stability that favour their use in industrial conditions (Thermal shock, chorine poisoning, water vapour, etc.). It has been made many efforts to enhanced redox abilities and surface acidities by the substitution of A or B cations [19,20], because the oxidation state at A-site or B-site can be modified. Further, anion vacancy could be produced by charge compensation. Kießling et al. [21] have shown that rare earth perovskites present high potentials as catalysts for the destruction of chloromethanes, chloroethanes and chloroethenes.

In this work the influence of Ce doping of $LaCoO_3$ perovskite in its physicochemical characteristics and thus in chlorobenzene combustion catalytic activity was widely studied. Additionally, the effect of the used synthesis method was analysed considering the importance of this step when large amount of catalysts must be synthetized for an industrial use. For this purpose, two methods will be employed at lab scale, the citrate and the reactive grinding methods. Both have been widely used in perovskites synthesis. The first one has been used because it provides solids with high surface area and purity [22]. The second one is well known to provide perovskites with high crystallinity at lower temperatures than other common techniques. Additionally, reactive grinding does not produce liquid effluents or hazardous vapours because single oxides are the perovskite precursors in agreement with green chemistry procedures [23]. The durability of catalysts was also studied in order to evaluate its possible industrial application.

2. Experimental

2.1 Catalysts preparation

$La_{1-x}Ce_xCoO_3$ (x = 0, 0.05, 0.1, 0.2, 0.5) perovskites were prepared by two different methods. In citrate method [24], metal nitrate solutions were added to a citric acid solution (10% in excess) and agitated during 15 min. The resulting solution was concentrated with a slowly evaporation in a rota vapour at 75 °C under vacuum until a gel was obtained. This gel was dried at 100 °C overnight in a vacuum stove, producing a solid amorphous precursor. The resulting precursor was milled and calcined in air at 700 °C for 2 h. The samples were named as CM_x, where CM: Citrate method and x: 0, 0.05, 0.1, 0.2, 0.5 corresponding to the Ce substitution level. In the reactive grinding method, the starting reagents were commercial La_2O_3 and CeO_2 (Sigma Aldhrich) and Co_3O_4 obtained from the thermal decomposition of cobalt acetate (Sigma Aldrich) calcined in air at 500 °C for 2 h. The milling process was carried out in a planetary ball milling (Fritsch Pulverissette 6) equipped with a cylindrical tungsten cabide vial (80 cm^3) and 15 mm diameter WC balls. The ball weigh-powder weight ratio was fixed at 10:1 and the rotation speed at 500 r/min. The milling time was 8 h and samples were finally calcined at 700 °C during 2 h. These samples were named: RG_x, RG considering reactive grinding method and x: 0, 0.05, 0.1, 0.2, 0.5 corresponding to the Ce substitution level.

2.2 Catalysts Characterization

BET specific surface area (SBET) of samples was calculated by the BET method. A Gemini V from Micromeritics apparatus was used. Samples were degassed overnight at 350 °C. X-ray diffraction (XRD) patterns were obtained with a Rigaku

(ULTIMA IV) diffractometer operated at 30 kV and 25 mA using Cu Kα radiation with Nickel filter (λ = 0.15418 nm). X-ray photoelectron spectroscopy (XPS) was recorded with a Multitecnic UniSpecs equipment with a dual X ray source of Mg/Al and a hemispheric analyzer PHOIBOS 150 was used to obtained XPS data. The pressure was kept under 29×10^{-8} mbar. The samples were previously reduced at 600 °C in 50 mL/min 5% of H_2/N_2 stream. Temperature programmed reduction (TPR) was performed in a quartz tubular reactor using a TCD detector. Samples of 100 mg were reduced with a mixture of 5 vol% H_2/N_2, at a total flow rate of 30 mL/min. The temperature was increased at a rate of 10 °C/min from room temperature to 700 °C.

2.3 Catalytic tests

The catalytic activity was made using a fixed-bed quartz reactor (12 mm diameter) at atmospheric pressure. Data were obtained in steady state. A sample of 200 mg (0.5–0.8 mm particle diameter) diluted with 1.5 g quartz particles of the same size was used. The feed was a mixture of 1000 ppm of chlorobenzene in air at a total flow rate of 200 mL/min. The reagents and exhaust gas were analyzed online by a Hewlett-Packard 5790 gas chromatograph equipped with a Carbowax 20 M / Chromosorb W column and a flame ionization detector (FID). The concentration of Cl_2 in the exhaust was analyzed by bubbling effluent stream in a 10 wt% NaOH solution. Then Cl_2 concentration was determined adding a known volume of this solution to a KI solution, followed by a titration of free iodine with a known concentration of $Na_2S_2O_3$ solution following the method reported elsewhere [24]. Stability tests were performed under the same conditions mentioned above. The reaction temperature was kept constant at 500 °C, which corresponds to total chlorobenzene conversion.

3. Results and discussion

3.1 Catalytic performance in chlorobenzene combustion

The samples synthetized in this work were evaluated in the catalytic combustion of chlorobenzene. Due to the high toxicity of dioxins and the need for laboratory safety, this compound was used as a model reagent in order to predict destruction behaviour of the synthetized catalysts. [3,25]. The catalytic activity results are shown in **Figs. 1, 2 and Table 1**. Fig. 1 shows the light off curves of chlorobenzene combustion for catalysts prepared by the reactive grinding method. As can be seen, catalysts presented a different behaviour as a function of temperature. At low reaction temperatures (lower than 350 °C) RG0, RG0.2 and RG0.5 presented a higher chlorobenzene combustion. However, at higher temperatures RG0.05 and RG0.1 became more active. Effectively, these catalysts presented the lower T50 and T90 values (Temperatures corresponding to 50% and 90% of total conversion). This different behaviour could indicate a different reaction mechanism which would involve the presence of intermediate compounds specially at low reaction temperature [26] [27] [28] [15]. The amount of Cl_2 determined at the end of the catalytic tests resulted similar to the theoretic value, 1.18×10^{-3} mol (Table 1). Additionally, the total carbon balance closed around 0% for all catalysts indicating that at high reaction temperature, chlorobenzene was converted completely to CO_2 and Cl_2. Fig. 2 shows the results of catalysts synthetized by the citrate method. It is interesting to note that at low temperature (lower than 300 °C) the chlorobenzene conversion increased in the following order: CM0<CM0.1<CM0.05<CM0.2<CM0.5. CM0.5 catalyst presented a higher conversion at low temperature but its behavior changed at high reaction temperature presenting the higher T50 and T90 values (Table 1). At high reaction temperatures the order changed as: CM0.5<CM0.1<CM0.2<CM0<CM0.05. The catalyst with the better catalytic activity was CM0.05. Cl_2 moles and carbon balance determined at the end of the reaction indicated total combustion in all cases.

Even if CM0.05 was slightly more active than RG0.05 there is not a marked effect of the synthesis method in the catalytic performance. The results were quite similar. However, Ce content presented a defined influence on catalysts activity with both methods. Only a small amount of Ce could enhance the activity of unsubstituted perovskite, specifically at high reaction temperature. Indeed, CM0.05 and RG0.05 presented lower reaction temperatures than CM0 and RG0. The addition of a higher content of Ce did not improve the catalysts performance. It could be deduced that a higher substitution degree of Ce (higher that 0.05) did not enhanced the catalytic activity of CM_x catalysts. Something similar happened with RG_x catalysts, even if the addition of Ce clearly improved the catalytic activity of RG0 catalyst, it could be deduced that a small value of x (x=0.05) was enough to improve the catalyst behavior. In fact, RG0.05 and RG0.1 were more active than RG0.2 and RG0.5 catalysts.

The activation energies of catalysts in the chlorobenzene combustion are summarized in **Table 1 and Fig. 3.** These values were calculated on the basis of a conversion less than 20%. The study of differential kinetics was conducted by assuming steady state before and after reaction. Then, a regression line was obtained by plotting ln k versus $1/T$, and activation energy (E_a) was calculated by Arrhenius equation. As it was expected lower activation energies were obtained for CM0.05 and RG0.05 catalysts, 38 and 33 kJ/mol respectively. Again, E_a increased with the increased of Ce content. The Ea values obtained with the catalysts prepared in this work resulted in the same order than those presented by Hao Huang and coworkers [1,3] with Ru/CeO_2 and VO_x/CeO_2 catalysts for catalytic combustion of chlorobenzene and also resulted similar to those presented by Gu and coworkers with WO_x/CeO_2 catalysts in the same reaction [29]. The turnover frequencies (TOF) were calculated as moles of converted chlorobenzene per hour and per surface area of catalyst according to the reaction rates at

200 °C. These values are also useful to describe the catalytic performance. As can be seen in Table 3, the higher TOF values were obtained with CM0.05 and RG0.05 catalysts, 6.1×10^{-3} and 5.57×10^{-3} mmol·m^2/h, respectively. These results confirmed the excellent catalytic performance of the above mentioned catalysts.

3.2 Catalysts characterization

A complete characterization of catalysts was made in order to determinate the physicochemical characteristics and its relationship with the catalytic results**. Table 2** shows the textural features of prepared catalysts. As can be observed, the synthesis method did not present a defined influence in catalysts surface area (SBET). Catalysts prepared by reactive grinding presented a higher SBET, however, the difference is not as marked as it would be expected. The citrate method has been extensible used in the synthesis of perovskites because it is known to provide solids with higher surface area in comparison with other methods like the ceramic ones [30]. In this case, probably, the SBET that the citrate method could provide due to the generated porosity would be comparable to SBET of catalysts prepared by reactive grinding due to the decrease of particle size during the milling process [23]. The partial doping of La with Ce produced a decrease of surface area, from 15 to 7 m^2/g for RG0 and RG0.05, respectively and from 11 to 4 m^2/g for CM0 and CM0.05, respectively. However, a higher substitution level did not significantly increase the surface area of catalysts. Evidently, the phases generated after the substitution did not present the same textural characteristics than the original perovskite. The different morphology of perovskites would also indicate structural differences in the samples. The XRD analysis confirms the presence of perovskite structure and, at high Ce content, the presence of CeO_2 and Co_3O_4 phases. This behaviour is similar in both series: CM and RG. The XRD patterns measured in step mode for all compounds were refined using the Rietveld method. Three phases

were used in the refinements: $La_{1-y}Ce_yCoO_3$ (S.G.: $R\bar{3}c$), CeO_2 (S.G.: $Fm\bar{3}m$) and Co_3O_4 (S.G.: $Fd\bar{3}m$). The Rietveld plots are showed in **Fig. 4(a, b)**. The main obtained parameters: cell parameters, crystallite size and strain and phase amounts, are summarized in **Table 3.** From these parameters, several crystal features can be used to understand the physicochemical and catalytic properties. The paramount parameter to know is the effective doping of Ce in the perovskite structure, however, this value is impossible to refine from X-ray pattern because La and Ce cations are virtually indistinguishable in terms of scattering factors. In spite of this, the Ce content in the perovskite structure also generates changes in the lattice (unit-cell volume and atomic distances) which can be used to estimate the Ce substitution. Regarding to the changes in the unit-cell volume, some aspects should be considered in terms of ionic radii; rLa^{3+}=0.136 nm, rCe^{3+}= 0.134 nm, rCe^{4+}=0.114 nm, rCo^{3+}=0.0745 nm and rCo^{2+}=0.061 nm [31]. The substitution of Ce^{3+} (or Ce^{4+}) instead La^{3+} cations induces a reduction in the unit-cell, but the presence of Ce^{4+} would induce Co^{2+} instead of Co^{3+} producing the opposite effect. The oxygen vacancies, which are likely in materials obtained with the presented methods, can increase the unit-cell volume. Similarly, the <(La/Ce)–O> and <Co–O> distances also are sensitive of Ce doping in the structure. In addition, the presence of CeO_2 and Co_3O_4 are indicative of incomplete doping and their amount can also be used to estimate the effective doping value. Thus, the nominal doping proposed in the synthesis and the obtained system can be understood as:

$$La_{1-x}Ce_xCoO_3 \rightarrow (1-x/1-y)\ La_{1-y}Ce_yCoO_3 + (x-y/1-y)CeO_2 + (x-y/3-3y)Co_3O_4$$

where x and y are the nominal and effective value of the Ce substitution. From this relationship is possible to estimate the effective value of Ce substitution (y) from the amount of each phase obtained in the Rietveld refinement. **Fig. 5** illustrates the unit-cell volume and interatomic distances vs x value. The dashed and dotted lines correspond to

a well-crystallized undoped phase ($LaCoO_3$). These plots reveal that the Ce doping in perovskite structure is more significant with the citrate method. It is known that textural properties, structure and composition of perovskites are strongly related to its redox property. Then, in order to investigate the reducibility of samples, H_2-TPR characterization was performed and the results are shown in **Fig. 6.** RG0 sample presented a reduction profile similar to those reported in literature for the same phase, $LaCoO_3$. The curve presents two main reduction zones, one of them from 300 to 500 °C and the other from 550 to 750 °C. The former corresponds to the reduction of Co^{3+} to Co^{2+}, while the latter is attributed to the reduction of Co^{2+} to Co^0 [32,33]. The addition of Ce induces changes in the reducibility of $LaCoO_3$ perovskite, evidenced by the shift of the first peak to lower temperatures, the overlapping of the two signals of the second peak and a shift of this peak to higher temperatures. The same was observed by other authors, [34–36] with the same perovskites. The deconvolution of this second signal is shown in order to enhance the visualization. At higher substitution levels, additional reduction signals could be detected from 500 to 600 °C. These additional signals could be assigned to the reduction of segregated CeO_2 species [37,38]. This fact is more evident in the case of RG0.2 and RG0.5. A similar behaviour was also observed in the case of CM_x samples, an overlapping of signals was detected in the rage of high reduction temperatures and additional reduction signals were detected specially with CM0.5 catalyst. These facts are in agreement with the higher amount of CeO_2 observed by DRX for x = 0.5 in both synthesis methods. Total H_2 consumptions of catalysts are displayed in **Table 2**. It is interesting to note that the H_2 consumption decrease with a small addition of Ce, from 3.41 to 3.05 mmol/g catalyst for RG0 and RG0.05 and from 3.65 to 3.21 mmol/g catalyst for CM0 and CM0.05 respectively. Assuming that the peaks at low substitution levels are attributed to the reduction of Co species, it could be

considered that the addition of Ce would facilitate the presence of Co^{2+} species in addition to Co^{3+} species, as observed by the Rietveld refinement. This redox pair Co^{2+}/Co^{3+} would be one of the positive factors that influence the catalytic performance. H_2 consumption increased with the increase in Ce substitution level for both synthesis methods. This could be due to the reduction of segregated CeO_2 species in addition to Co species in accordance with the reduction signals observed. Evidently, the presence of segregated CeO_2 at the surface of high substitution level catalysts generated low active catalytic sites. In order to study the disposition of cations at the surface of catalysts which is the responsible of the catalytic behaviour, the XPS analysis was carried out and the profiles of Ce 3d, Co 3d and O 1s are shown in **Figs. 7–9**, respectively. The main XPS data are listed in **Table 4.** Ce3d spectra could be deconvoluted into eight peaks assigned to four pairs of spin-orbit doublets (**Fig. 7).** The peaks named as u and v are characteristics of $Ce3d_{3/2}$ and Ce $3d_{5/2}$ multiples, respectively. The doublet *u*' (902.9 eV) and *v*' (883.4 eV) refers to Ce^{3+} 3d final state, while the peaks *v* (881.8 eV), *v*'' (887.9 eV), *v*'''(897.5 eV), *u* (900.1 eV), *u*''(906.6 eV), and *u*'''(916.1 eV) feature Ce^{4+} [36]. As can be seen in **Table 4**, the Ce^{3+}/Ce^{4+} ratio decreased from 1.6 to 1.1 for RG0.05 and RG0.5, respectively. A similar effect can be observed with CM catalysts. These results are in line with RTP results, the segregation of CeO_2 is also evident at the surface of catalysts with higher substitution levels. **Table 4** shows the binding energies of Co $2p_{1/2}$ and Co $2p_{3/2}$. It is known that the difference between these two levels is about 15.1 eV which indicates Co^{3+} presence[39,40]. For all catalysts prepared by both methods in this work, the difference is higher than 15.1 eV which indicates that some Co^{2+} (where the difference is about 16 eV) coexists with Co^{3+}. The Co $2p_{3/2}$ peak is deconvoluted into two components at 779 and 781 eV, assignable to surface Co^{2+} and Co^{3+} species respectively (**Fig. 8**). The $Co^{2+/}Co^{3+}$ ratio (see **Table 4**) increased from

0.31 to 0.44 for RG0 and RG0.05, respectively, and from 0.27 to 0.39 for CM0 and CM0.05 catalysts. The Co^{2+}/Co^{3+} ratio decreased with a higher Ce substitution levels. This could be attributed to the fact that the valence state of some Co cations in B-sites changes from Co^{3+} to Co^{2+} in order to maintain the electronic neutrality when Ce is introduced into the perovskite structure. The higher presence of this Co^{2+}/Co^{3+} redox pair in RG0.05 and CM0.05 catalysts, would the responsible of its higher catalytic activity in chlorobenzene combustion. It is widely known that the catalytic activity of perovskite oxides is related to transition metal ions oxidation states, the amount of non-stoichiometric oxygen and the structural defects of lattice. The nature of VOC molecule to be oxidised will define which of these aspects will be more relevant for the catalytic performance and will give an idea about the reaction mechanism. Chlorobenzene is generally adsorbed and dissociated on surface active sites via a nucleophilic attack on C–Cl bond. Then the adsorbed species react with active oxygen species to produce CO_2, and H_2O. Simultaneously, the dissociative Cl^- species adsorbed are oxidized into Cl_2 by surface reactive oxygen species through the Deacon reaction ($2HCl + O_2 \rightarrow Cl_2 + H_2O$). Finally, the consumed oxygen species are replenished by the gas-phase oxygen adsorbed on the oxygen vacancies. Thus, it is of great importance to study the surface oxygen in order to understand the catalysts behaviour. As shown in **Fig. 9,** the O1s spectra could be deconvoluted into two components. The peak at high binding energies (531.3–532.2 eV) corresponds to the surface adsorbed oxygen (Oads) such as O_2^{2-} or O^- and hydroxyl OH^-, while the peak at low binding energies (529.2–530.0 eV) is attributed to lattice oxygen O^{2-} (Olat)[41,42]. As it can be observed in **Table 4** Oad/Olat ratio increased with a small addition of Ce from 0.50 to 0.86 for RG0 and RG0.05 and from 0,78 to 0.84 for CM0 and CM0.05 respectively. At higher Ce substitution levels this value decreased indicating that the incorporation of cerium in the perovskite

structure can significantly increase the surface concentration of adsorbed oxygen. Effectively, catalysts with the higher Oad/Olat ratio, RG0.05 and CM0.05, presented a higher catalytic activity that those catalysts with an excess of cerium at the surface as segregated CeO_2. As mentioned above, the higher concentration of adsorbed oxygen in these catalysts would favour the HCl oxidation reaction by the Deacon Process, which would lead to a higher removal of Cl species from the catalyst surface.

3.3 Catalysts stability and characterization of used samples

The main problem to solve during chlorinated combustion process is the deactivation of catalysts due to the presence of Cl species on surface active sites. Thus it is essential to investigate catalysts stability since it is an important indicator for determining whether the catalysts can be used in the industry. Therefore, the durability of CM0.05 and RG0.05 catalysts was studied. **Fig. 10** shows the chlorobenzene conversion evolution time on stream at different temperatures corresponding to 80% and 100% of chlorobenzene conversion with each catalyst. The selected temperatures were 380 and 420 °C for the stability of CM0.05 and RG0.05 respectively for a conversion level of 80% and 500 °C for both catalysts in the case of 100% of chlorobenzene conversion. As it was expected the stability of both catalysts was lower at low reaction temperature. At 80% conversion level both catalysts remained stable during the first 24 h and then, chlorobenzene conversion started to decrease up to 10% when the reaction time was 38 h. A different behaviour was observed at higher reaction temperature. As can be seen both catalysts showed an excellent stability during the first 40 h in the case of CM0.05 and during 45 h in the case of RG0.05 catalyst keeping 100% of chlorobenzene conversion. The comparison of catalysts stability presented in reported literature is difficult due to the differences in experimental conditions.

However, the stability of catalysts presented in this work is higher than that presented by Deng et al. [37] with cobalt based mixed oxides derived from layered double hydroxides with a space velocity of 30000 mL/(Lg·h) and 1000 ppm of Chlorobenzene. Wang and col, [43] presented a stability test of 20 h in chlorobenzene combustion using a space velocity of 20000 h^{-1} and 660 ppm. Some other authors, [44] reported stability tests with the addition of 5% water vapour and showed the stability during 10 h with 500 ppm of chlorobenzene and a sapace velocity of 15000 ml L/(g·h).

It is worthy mentioned that both catalysts presented in this work started to deactivate and chlorobenzene conversion decreased to almost 50% after 52 h on stream at 500°C. The amount of Cl_2 determined at the end of reaction tests at 500 °C were 0.79 $\times10^{-3}$ and 0.65×10^{-3} moles for RG0.05 and CM0.05 catalysts, respectively. While the amount of Cl_2 at the end of reaction test performed at lower temperatures were 0.51×10^{-3} and 0.47×10^{-3} mol for RG0.05 and CM0.05, respectively. In all cases these values resulted lower than the theoretical one, 1.18×10^{-3} mol. A higher difference among these values was observed at low reaction temperature. Carbon balance was also determined and it closed almost to 0% in both catalysts at 500 °C, but at lower reaction temperatures it closed to 1.32% and 2.4% for RG0.05 and CM0.05 catalysts, respectively. The low amount of Cl_2 detected could indicate that some by-products as chlorinated hydrocarbons were formed during the combustion process. This fact is more probable at low reaction temperature considering the amount of Cl and carbon balance at the end of reaction test. However, carbon balance obtained at 500 °C revealed that no additional carbon products were obtain, so this fact is unprovable at this reaction temperature. Therefore, the decrease of activity could be attributed to the adsorption of Cl species on the surface of catalysts that may block the active sites as it was previously found by several researchers [45–48]. At lower reaction temperatures, the formation of

some by-products at the surface catalysts would be the responsible of catalysts deactivation. Clearly, at low temperature the removal of Cl species is more difficult than it is at higher temperature[49]. It interesting to note, that even though these results are interesting in order to study the causes of deactivation of catalysts, the stability test at 500 °C corresponding to a 100% of chlorobenzene conversion is more relevant if a possible real catalytic application is considered, where a complete destruction of chlorobenzene is needed. The diffraction patterns of used catalysts are presented in **Fig. 11.** As can be seen, the diffractograms obtained after the stability tests are quite different to the ones of fresh catalysts. The intensity of diffraction peaks corresponding to the perovskite phase (PDF 00-048-0123) decreased notably and additional peaks could be detected in all catalysts which were identified as CeO_2 (PDF 00-048-0123), Co_3O_4 (PDF 96-900-5888) and LaOCl (PDF 96-900-9171) phases. These results explain the drop in chlorobenzene conversion. Evidently Cl species adsorb on catalysts surface preferentially on La cations, due to its basic character, forming the LaOCl compound. Consequently, the perovskite phase is destroyed and is decomposed in the corresponding simple oxides. The same was reported by Sinkin et al. [50] with $LaCoO_3$ perovskites used in the combustion of CH_2Cl_2, $CHCl_3$ and CCl_4.

Evidently, the excellent activity provided by the Co^{2+}/Co^{3+} and Ce^{3+}/Ce^{4+} pair redox and the oxygen vacancies present in the perovskite decreases with time on stream after around 45 hs due to the partial surface deactivation of perovskite structure by means of chlorine incorporation. However, this fact probably is reversible because it is possible to recover catalysts introducing water vapour, since water would depress Deacon reaction and promote the removal of Cl species [51]. Besides, we could demonstrate in this article that a reactive grinding process would be useful to recover the perovskite structure from it corresponding oxides. Several studies about the

regeneration of catalysts taking into account the process steps mentioned above are being developed and will be published elsewhere.

Conclusions

In this work, a series of Ce-doped $LaCoO_3$ perovskites catalysts were synthetized by two methods, the citrate and the reactive grinding methods. Both methods provided active catalysts in the studied reaction reaching only total combustion products, CO_2, Cl_2 and H_2O at high reaction temperatures. The most active catalysts were those with the low substitution level (x=0.05) synthetized by both methods. Thus, this fact results interesting considering the possibility of a future scale up. The reactive grinding method could be easily reproduced in large scale with zero contaminant effluents. The Ce-doping in the original perovskite structure was observed up to a level of x=0.05. For higher substitutions levels, segregated CeO_2 was detected in all catalysts. The insertion of Ce favored the presence of $Co^{2+/}Co^{3+}$ and $Ce^{3+/}Ce^{4+}$ redox pairs and a higher content of oxygen vacancies that enhance the catalytic performance in chlorobenzene combustion based in differential kinetics studies. Finally, durability tests were carried out in order to determinate the stability of catalysts on time on stream. It was demonstrated that catalysts presented a stable catalytic performance with 100% of chlorobenzene conversion during 45 h. After that time, the catalysts started to deactivate due to the adsorption of Cl species on catalyst surface. Finally, all results support the promising properties of $La_{1-x}Ce_xCoO_3$ with x = 0.05 as a suitable catalyst to treat chlorinated volatile organic compounds of industrial waste.

Acknowledgements

The financial support from Universidad Nacional de San Luis, CONICET, ANPCyT is gratefully acknowledged.

References

1. BB Huang, C Lei, CH Wei, GM Zeng. Chlorinated volatile organic compounds (Cl-VOCs) in environment - sources, potential human health impacts, and current remediation technologies. *Environ Int*. 2014;71:118.
2. De Pedro ZM, Gómez-Sainero LM, González-Serrano E, Rodríguez JJ. Gas-phase hydrodechlorination of dichloromethane at low concentrations with palladium/carbon catalysts. *Ind Eng Chem Res*. 2006;45(23):7760.
3. H Huang, YF Gu, J Zhao, XY Wang. Catalytic combustion of chlorobenzene over VO_x/CeO_2 catalysts. *J Catal*. 2015;326:54.
4. Vu VH, Belkouch J, Ould-Dris A, Taouk B. Removal of hazardous chlorinated VOCs over Mn-Cu mixed oxide based catalyst. *J Hazard Mater*. 2009;169(1-3):758.
5. J Xiong, QQ Wu, XL Mei, J Liu, YC Wei, Z Zhao, et al. Fabrication of Spinel-Type $Pd_xCo_{3-x}O_4$ Binary Active Sites on 3D Ordered Meso-macroporous Ce-Zr-O2 with Enhanced Activity for Catalytic Soot Oxidation. *ACS Catal*. 2018;8(9):7915.
6. XX Dai, WY Jiang, WL Wang, XL Weng, Y Shang, YH Xue, et al. Supercritical water syntheses of transition metal-doped CeO_2 nano-catalysts for selective catalytic reduction of NO by CO: An *in situ* diffuse reflectance Fourier transform infrared spectroscopy study. *Cuihua Xuebao/Chin J Catal*. 2018;39(4):728.
7. Gannoun C, Turki A, Kochkar H, R Delaigle, EM Gaigneaux. Elaboration and characterization of sulfated and unsulfated V_2O_5/TiO_2 nanotubes catalysts for chlorobenzene total oxidation. *Appl Catal B Environ*. 2014;147:58.
8. Scirè S, Minicò S, Crisafulli C. Pt catalysts supported on H-type zeolites for the catalytic combustion of chlorobenzene. *Appl Catal B Environ*. 2003;45(2):117.

9. W Deng, QG Dai, YJ Lao, BB Shi. Low temperature catalytic combustion of 1,2-dichlorobenzene over CeO_2–TiO_2 mixed oxide catalysts. *Appl Catal B Environ*. 2016;181:848.

10. Zuo SF, Ding ML, Tong J, Feng LC, Qi CZ. Study on the preparation and characterization of a titanium-pillared clay-supported CrCe catalyst and its application to the degradation of a low concentration of chlorobenzene. *Appl Clay Sci*. 2015;105-106:118.

11. Zhang LL, Liu SY, Wang GY, Zhang JX. Catalytic combustion of dichloromethane over NaFAU and HFAU zeolites: A combined experimental and theoretical study. *React Kinet Mech Catal*. 2014;112(1):249.

12. Wang XY, Kang Q, Li D. Catalytic combustion of chlorobenzene over MnO_x-CeO_2 mixed oxide catalysts. *Appl Catal B Environ*. 2009;86(3-4):166.

13. Topka P, Delaigle R, Kaluža L, Gaigneaux EM. Performance of platinum and gold catalysts supported on ceria-zirconia mixed oxide in the oxidation of chlorobenzene. *Catal Today*. 2015;253:172.

14. YL Gu, YX Yang, YM Qiu, KP Sun, XL Xu. Combustion of dichloromethane using copper-manganese oxides supported on zirconium modified titanium-aluminum catalysts. *Catal Commun*. 2010;12(4):277.

15. Sun PF, Wang WL, Dai XX, Weng XL, Wu ZB. Mechanism study on catalytic oxidation of chlorobenzene over $Mn_xCe_{1-x}O_2$/H-ZSM5 catalysts under dry and humid conditions. *Appl Catal B Environ*. 2016;198:389.

16. Dai Y, Wang XY, Dai QG, Li D. Effect of Ce and La on the structure and activity of MnO_x catalyst in catalytic combustion of chlorobenzene. *Appl Catal B Environ*. 2012;111-112:141.

17. Yang P, Yang SS, Shi ZN, Meng ZH, Zhou RX. Deep oxidation of chlorinated

VOCs over CeO_2-based transition metal mixed oxide catalysts. *Appl Catal B Environ*. 2015;162:227.

18. Chen HH, Zhang HP, Yan Y. Gradient porous Co-Cu-Mn mixed oxides modified ZSM-5 membranes as high efficiency catalyst for the catalytic oxidation of isopropanol. *Chem Eng Sci*. 2014;111:313.

19. YJ Lu, QG Dai, XY Wang. Catalytic combustion of chlorobenzene on modified $LaMnO_3$ catalysts. *Catal Commun*. 2014;54:114.

20. Zhang CH, Wang C, Zhan WC, Guo YL, Guo Y, Lu GZ, et al. Catalytic oxidation of vinyl chloride emission over $LaMnO_3$ and $LaB_{0.2}Mn_{0.8}O_3$ (B=Co, Ni, Fe) catalysts. *Appl Catal B Environ*. 2013;129:509.

21. Kießling D, Schneider R, Kraak P, Haftendorn M, Wendt G. Perovskite-type oxides - Catalysts for the total oxidation of chlorinated hydrocarbons. *Appl Catal B Environ*. 1998;19(2):143.

22. Cifà F, Dinka P, Viparelli P, Lancione S, Benedetti G, Villa PL, et al. Catalysts based on $BaZrO_3$ with different elements incorporated in the structure I: $BaZr_{1-x}Pd_xO_3$ systems for total oxidation. *Appl Catal B Environ*. 2003;46(3):463.

23. Kaliaguine S, Szabo V, Van Neste A, Gallot JE, Bassir M, Muzychuk R. Perovskite-Type Oxides Synthesized by Reactive Grinding. *JMNM Electrochem Chem React Amorph Nanocrystalline Mater*. 2001;11:39.

24. Courty P, Ajot H, Marcilly C, Delmon B. Oxydes mixtes ou en solution solide sous forme très divisée obtenus par décomposition thermique de précurseurs amorphes. *Powder Technol*. 1973;7(1):21.

25. F He, JQ Luo, ST Liu. Novel metal loaded KIT-6 catalysts and their applications in the catalytic combustion of chlorobenzene. *Chem Eng J*. 2016;294:362.

26. Wang J, Wang X, Liu XL, Zeng JL, Guo YY, Zhu TY. Kinetics and mechanism

study on catalytic oxidation of chlorobenzene over V_2O_5/TiO_2 catalysts. *J Mol Catal A Chem*. 2015;402:1.

27. QG Dai, SX Bai, XY Wang, GZ Lu. Catalytic combustion of chlorobenzene over Ru-doped ceria catalysts: Mechanism study. *Appl Catal B Environ*. 2013;129:580.

28. Finocchio E, Ramis G, Busca G. A study on catalytic combustion of chlorobenzenes. *Catal Today*. 2011;169(1):3.

29. YF Gu, T Cai, XH Gao, HQ Xia, W Sun, J Zhao, et al. Catalytic combustion of chlorinated aromatics over WO_x/CeO_2 catalysts at low temperature. *Appl Catal B Environ*. 2019;248:264.

30. Athayde DD, Souza DF, Silva AMA, Vasconcelos D, Nunes EHM, da Diniz CJC, et al. Review of perovskite ceramic synthesis and membrane preparation methods. *Ceram Int*. 2016;42(6):6555.

31. Shannon RD. Revised effective ionic radii and systematic studies of interatomic distances in halides and chalcogenides. *Acta Crystallogr Sect A*. 1976;32(5):751.

32. Lago R, Bini G, Peña MA, Fierro JLG. Partial oxidation of methane to synthesis gas using $LnCoO_3$ perovskites as catalyst precursors. *Stud Surf Sci Catal*. 1997;110:721.

33. Fierro JLG. Structure and composition of perovskite surface in relation to adsorption and catalytic properties. *Catal Today*. 1990;8(2):153.

34. R You, YX Zhang, DS Liu, M Meng, Z Jiang, S Zhang, Yuying Huang. A series of ceria supported lean-burn nOx trap catalysts $LaCoO_3/K_2CO_3/CeO_2$ using perovskite as active component. *Chem Eng J*. 2015;260:357.

35. JJ Zhu, YX Zhao, DH Tang, Z Zhao, SAC Carabineiro. Aerobic selective oxidation of alcohols using $La_{1-x}Ce_xCoO_3$ perovskite catalysts. *J Catal*.

2016;340:41.

36. Ansari AA, Adil SF, Alam M, Ahmad N, Assal ME, Labis JP, et al. Catalytic performance of the Ce-doped $LaCoO_3$ perovskite nanoparticles. *Sci Rep*. 2020;10(1):1.

37. SS Lia, J Deng, Y Dan, L Xiong, JL Wang, YQ Chen. Designed synthesis of highly active CeO_2-ZrO_2-Al_2O_3 support materials with optimized surface property for Pd-only three-way catalysts. *Appl Surf Sci*. 2020;506:144866.

38. Romeo M, Bak K, El Fallah J, Le Normand F, Hilaire L. XPS Study of the reduction of cerium dioxide. *Surf Interface Anal*. 1993;20(6):508.

39. Merino NA, Barbero BP, Grange P, Cadús LE. $La_{1-x}Ca_xCoO_3$ perovskite-type oxides: Preparation, characterisation, stability, and catalytic potentiality for the total oxidation of propane. *J Catal*. 2005;231(1):232.

40. X Wang, BF Jin, RX Feng, W Liu, D Weng, XD Wu, et al. A robust core-shell silver soot oxidation catalyst driven by Co_3O_4: Effect of tandem oxygen delivery and Co_3O_4-CeO_2 synergy. *Appl Catal B Environ*. 2019;250(December 2018):132.

41. HZ Chang, XY Chen, JH Li, L Ma, CZ Wang, CX Liu, et al. Improvement of activity and SO_2 tolerance of Sn-modified MnO_x-CeO_2 catalysts for NH_3-SCR at low temperatures. *Environ Sci Technol*. 2013;47(10):5294.

42. SF Song, C Zhang, YK Lou, YJ Wu, L Wang, YL Guo, et al. Effects of water on CO catalytic oxidation over Pd/CeO_2. *J Rare Earths*. 2020;38(8):891.

43. Wang Y, Wang G, Deng W, Han J. Study on the structure-activity relationship of Fe-Mn oxide catalysts for chlorobenzene catalytic combustion. *Chem Eng J*. 2020;395.

44. XJ Zhang, YH Wei, ZX Song, W Liu, CX Gao, JW Luo. Silicotungstic acid modified CeO_2 catalyst with high stability for the catalytic combustion of

chlorobenzene. *Chemosphere*. 2021;263:128129.

45. GY Long, MX Chen, YJ Li, JF Ding, RZ Sun, YF Zhou, et al. One-pot synthesis of monolithic Mn-Ce-Zr ternary mixed oxides catalyst for the catalytic combustion of chlorobenzene. *Chem Eng J*. 2019;360:964.

46. He C, Xu BT, Shi JW, Qiao NL, Hao ZP, Zhao JL. Catalytic destruction of chlorobenzene over mesoporous $ACeO_x$ (A = Co, Cu, Fe, Mn, or Zr) composites prepared by inorganic metal precursor spontaneous precipitation. *Fuel Process Technol*. 2015;130(C):179.

47. QG Dai, XY Wang, GZ Lu. Low-temperature catalytic combustion of trichloroethylene over cerium oxide and catalyst deactivation. *Appl Catal B Environ*. 2008;81(3-4):192.

48. Lichtenberger J, Amiridis MD. Catalytic oxidation of chlorinated benzenes over V_2O_5/TiO_2 catalysts. *J Catal*. 2004;223(2):296.

49. W Deng, QX Tang, SS Huang, L Zhang, ZY Jia, LM Guo. Low temperature catalytic combustion of chlorobenzene over cobalt based mixed oxides derived from layered double hydroxides. *Appl Catal B Environ*. 2020;278:119336.

50. Sinquin G, Petit C, Libs S, Hindermann JP, Kiennemann A. Catalytic destruction of chlorinated C1 volatile organic compounds (CVOCs) reactivity, oxidation and hydrolysis mechanisms. *Appl Catal B Environ*. 2000;27(2):105.

51. GY Long, MX Chen, YJ Li, JF Ding, RZ Sun, YF Zhou, et al. One-pot synthesis of monolithic Mn-Ce-Zr ternary mixed oxides catalyst for the catalytic combustion of chlorobenzene. *Chem Eng J*. 2019;(July):964.

Table 1. Catalytic activity results

Catalyst	T_{50}	T_{90}	Total carbon balance (%)	$n(Cl_2)$ (mol) as a reaction product	Activation Energies (E_a) (kJ/mol)	TOF[a] (mmol/(m^2·h))
RG 0	454	491	0.90	1.02×10^{-3}	42.55	1.86×10^{-3}
RG 0.05	377	434	0.30	0.94×10^{-3}	33.69	5.57×10^{-3}
RG 0.1	389	422	0.30	1.15×10^{-3}	71.77	2.19×10^{-3}
RG 0.2	438	476	0.80	1.22×10^{-3}	100.68	2.20×10^{-3}
RG 0.5	421	473	0.60	1.15×10^{-3}	95.46	1.95×10^{-3}
CM 0	356	439	0.60	1.17×10^{-3}	44.33	1.82×10^{-3}
CM 0.05	313	425	0.40	1.22×10^{-3}	38.22	6.10×10^{-3}
CM 0.1	385	456	0.50	1.08×10^{-3}	84.95	5.40×10^{-3}
CM 0.2	325	461	0.70	1.16×10^{-3}	111.33	4.25×10^{-3}
CM 0.5	425	474	0.80	1.18×10^{-3}	112.97	3.16×10^{-3}

a TOF calculated as moles of converted chlorobenzene per hour based on catalyst surface area

Table 2. SBET, pore size and H_2 consumption from RTP results

Catalyst	BET surface (m^2/g)	Pore Size (nm)	H_2 consumption ($\times10^{-4}$ mol/gcat)
RG0	15	3.442	3.40
RG0.05	7	3.425	3.05
RG0.1	8	7.348	3.14
RG0.2	7	5.864	3.64
RG0.5	6	3.588	3.86
CM0	11	7.699	3.65
CM0.05	4	13.607	3.21
CM0.1	5	12.819	3.33
CM0.2	4	12.306	3.68
CM0.5	6	10.097	4.19

Table 3 Parameters obtained by Rietveld Method.

a) Reactive Grinding
Ce content

Ce-doped $LaCoO_3$	**0%**	**5%**	**10%**	**20%**	**50%**
a (nm)	0.54357(4)	0.54354(3)	0.54361(4)	0.54313(6)	0.54336(8)
c (nm)	1.3137(1)	1.3136(1)	1.3146(1)	1.3159(2)	1.3230(4)
V(nm^3)	0.33616(5)	0.33609(4)	0.33642(5)	0.33615(7)	0.3383(1)
Amount (%*P*/*P*)					
$La_{1-y}Ce_yCoO_3$	100	100	89(2)	89(3)	37(1)
CeO_2	-	-	4.1(4)	5(1)	43(1)
Co_3O_4	-	-	5.6(8)	6(2)	20(2)
Crystallite size (nm)					
$La_{1-y}Ce_yCoO3$	51.9	55.1	32.5	20.8	17.9
CeO_2	-	-	14.4	11.9	11.5
Co_3O_4	-	-	37.4	25.2	9.3
b) Citrate method					
Ce content					
Ce-doped $LaCoO_3$	**0%**	**5%**	**10%**	**20%**	**50%**
a (nm)	0.54360(6)	0.54303(7)	0.54295(7)	0.54258(3)	0.5439(2)
c (nm)	1.3121(2)	1.3127(2)	1.3152(2)	1.3210(1)	1.3156(6)
V (nm^3)	0.33578(6)	0.33523(7)	0.33578(8)	0.33680(4)	0.3371(2)
Amount (%*P*/*P*)					
$La_{1-y}Ce_yCoO_3$	100	100	95.1	95(1)	47(3)
CeO_2	-	-	-	5.0(5)	46(2)
Co_3O_4	-	-	-	0.3(1)	7(1)
Crystallite size (nm)					
$La_{1-y}Ce_yCoO_3$	35.3	72.6	47.9	34.4	19.9
CeO_2	-	-	-	7.0	9.5
Co_3O_4	-	-	-	-	-

Table 4 XPS results

Catalyst	**O_{add}/O_{latt}**	**Ce^{3+}/Ce^{4+}**	**Co^{2+}/Co^{3+}**	**Energy difference (eV) Co^{2+}/Co^{3+}**
RG0	0.50	-----	0.31	15.47
RG0.05	0.86	1.60	0.44	15.47
RG0.1	0.62	1.40	0.12	15.36
RG0.2	0.62	1.50	0.12	15.36
RG0.5	0.29	1.10	0.14	15.36
CM0	0.78	-----	0.27	15.12
CM0.05	0.84	1.03	0.39	15.00
CM0.1	0.62	0.89	0.32	15.24
CM0.2	0.35	0.99	0.29	15.12
CM0.5	0.41	0.91	0.31	15.24

Figure Captions

Figure 1. Catalytic performance of RG catalysts in Chlorobenzene combustion reaction.

Figure 2. Catalytic behaviour of CM catalyst in Chlorobenzene combustion reaction.

Figure 3. Arrhenius plot for rate constant of chlorobenzene conversion with RG (a) and CM catalysts (b).

Figure 4. XRD patterns with Rietveld refinements plots for RG catalysts.

Figure 5. XRD patterns with Rietveld refinements plots for CM catalysts.

Figure 6. (a) Unit-cell volume vs *x* value; (b) Interatomic distances vs *x* value.

Figure 7. H_2-temperature programed reduction (H_2-TPR) profiles of RG (a) and CM (b) catalysts.

Figure 8. XPS spectra of Ce 3d for RG (a) and CM (b) catalysts

Figure 9. XPS spectra of Co2p for RG (a) and CM (b) catalysts

Figure 10. XPS spectra of O1s for RG (a) and CM (b) catalysts

Figure 11. Stability tests. Chlorobenzene conversion evolution on time on stream.

Figure 12. XRD patterns of RG0.05 and CM0.05 catalysts before and after the stability tests at 80% and 100% of chlorobenzene conversion. • $LaCoO_3$-PDF 00-048-0123; ▲ CeO_2-PDF 96-900-9009; ★ Co_3O_4-PDF 96-900-5888; □ LaOCl-PDF 96-900-9171.

Graphical Abstract Description

Ce-doped $LaCoO_3$ perovskites catalysts prepared by two different methods (citrate and reactive grinding) present an excellent catalytic activity and stability in the chlorobenzene total combustion reaction with zero formation of by-products.

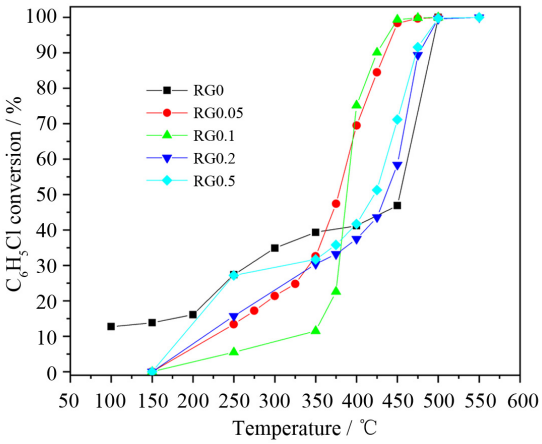

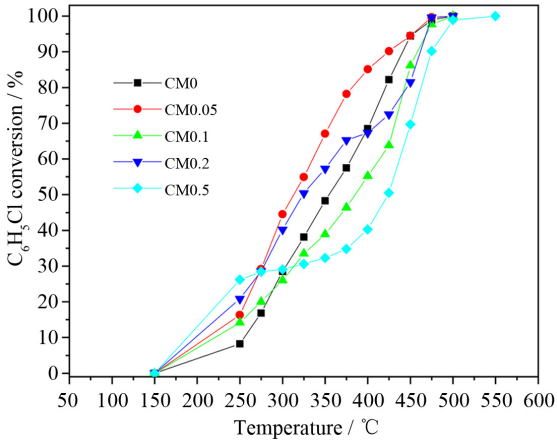

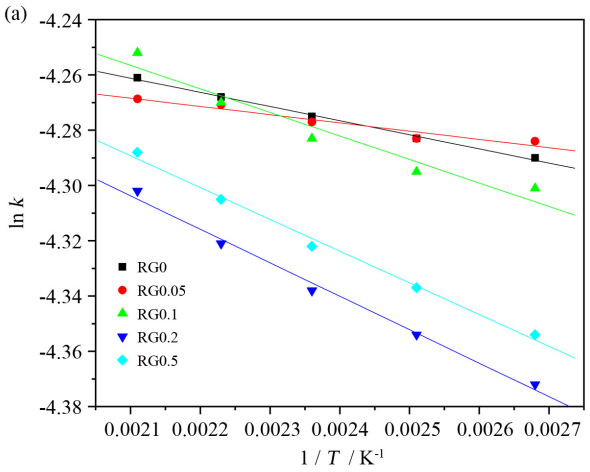

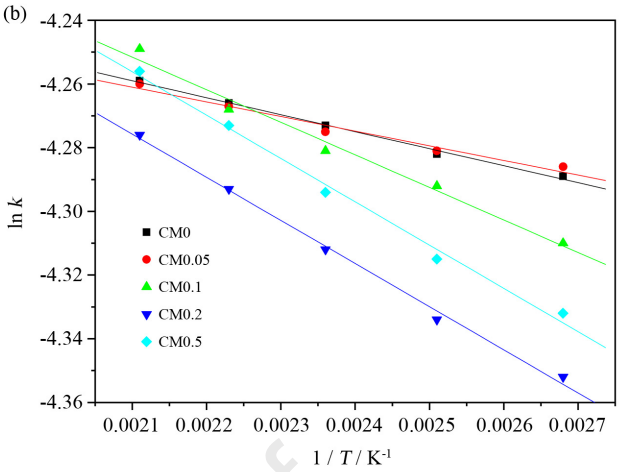

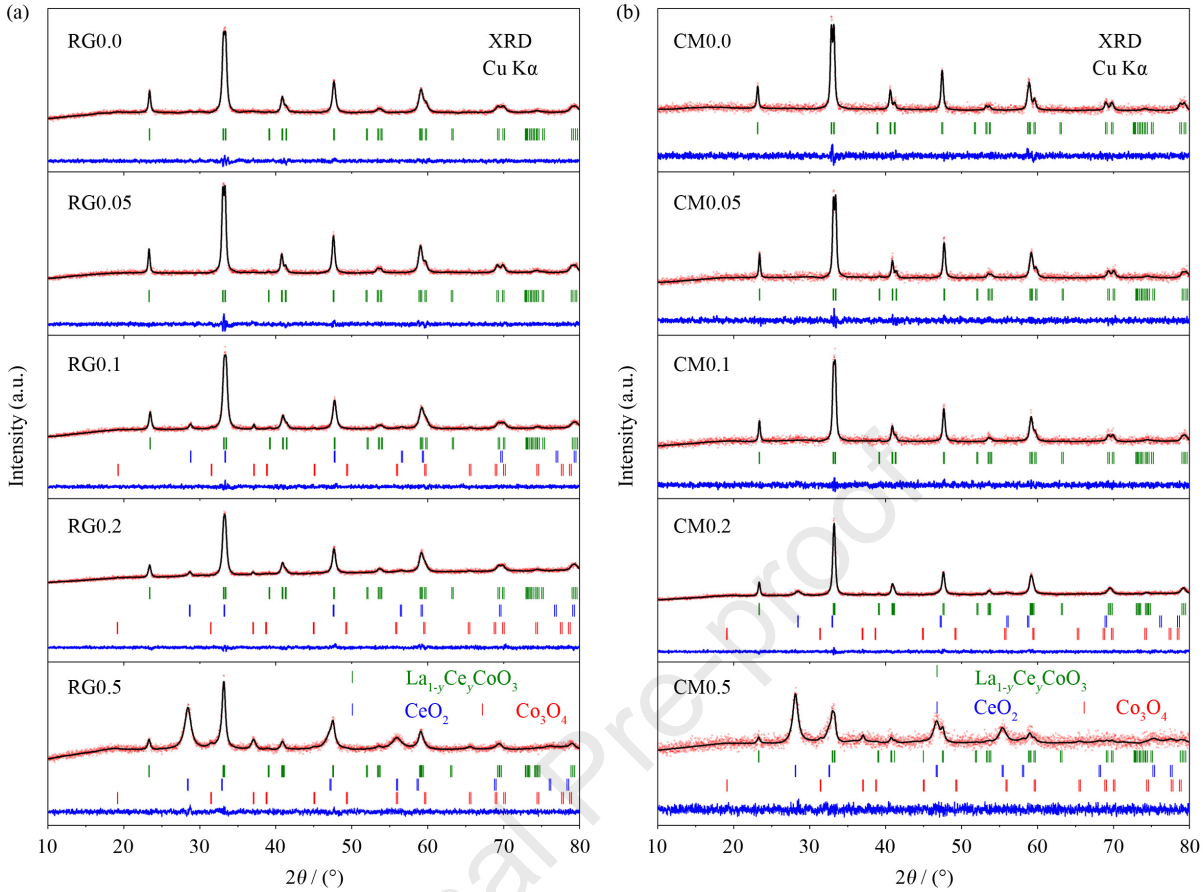

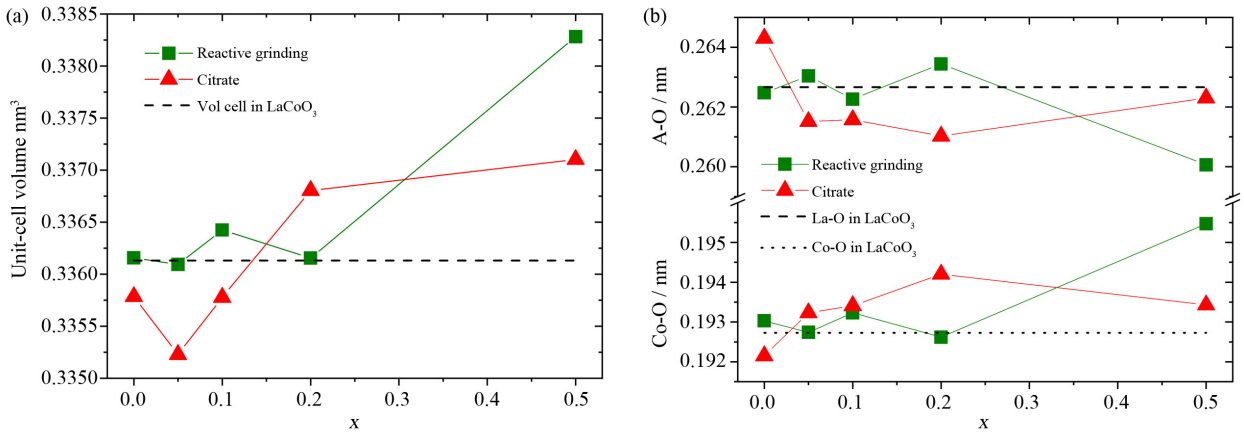

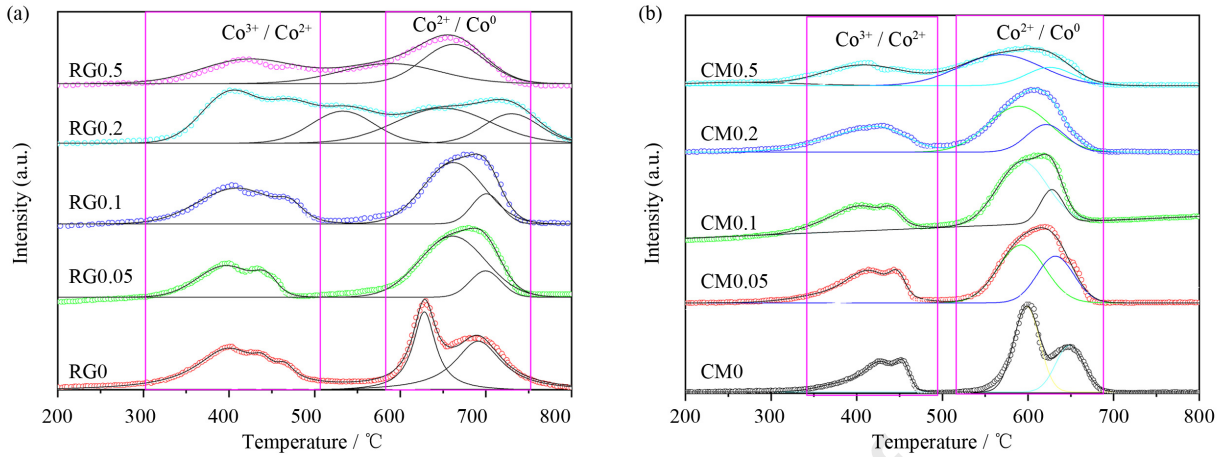

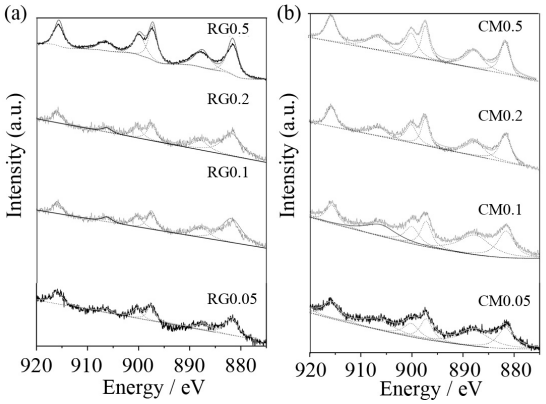

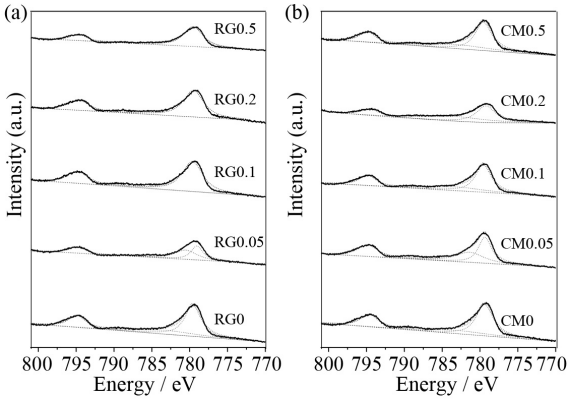

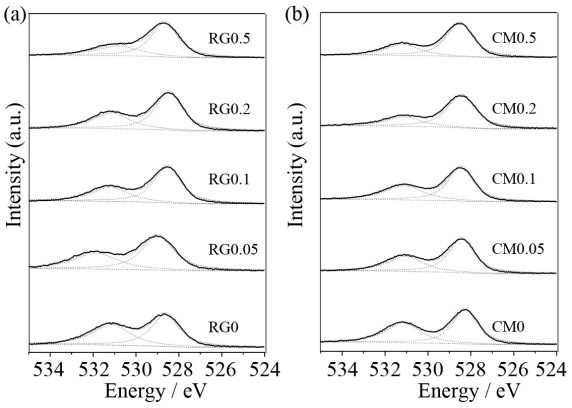

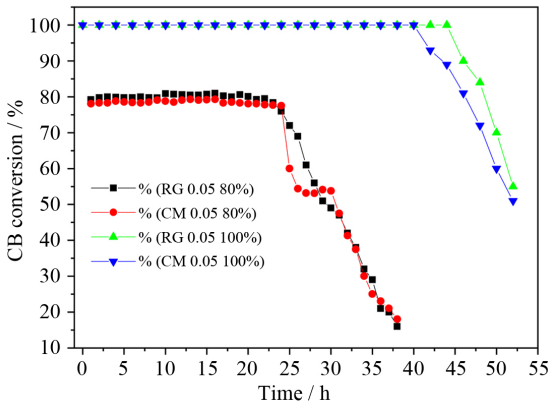

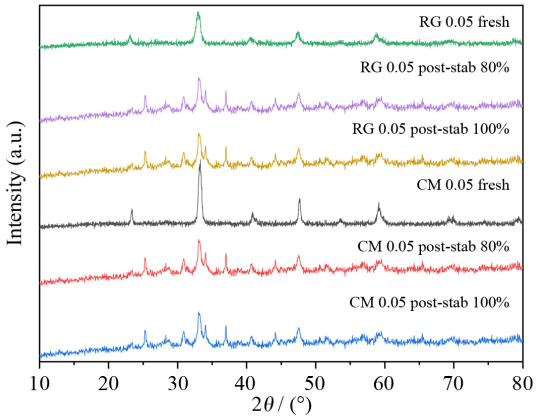

Highlights

- A green synthesis method was feasible to use in order to obtain active catalysts.
- The redox combination of the substituted catalysts increases the catalytic activity.
- Catalysts oxidize chlorobenzene to its total oxidation products, without final intermediates.
- Differential kinetic studies corroborated the catalytic capacity of the catalysts obtained.
- Samples presented an excellent stability during 45 hs time on stream

Declaration of interests

☒ The authors declare that they have no known competing financial interests or personal relationships that could have appeared to influence the work reported in this paper.

☐The authors declare the following financial interests/personal relationships which may be considered as potential competing interests: